Check for updates

A sensitive and selective fluorescent probe for hydrazine with a unique nonaromatic fluorophore†

Jian Liu,[a] Tao Li,[a] Shun Wang,[a] Qingrong Qi,[b] Hang Song, [ID][a] Zicheng Li,[a] Li Yang*[c] and Wencai Huang [ID] *[a]

To achieve sensitive, selective and facile detection of hydrazine in environmental and biological systems, a fluorescent probe (**Che-Dcv**) with a unique nonaromatic fluorophore was developed. Upon hydrazine addition in 20% DMSO−PBS buffer (pH = 7.4, 10 mM, v/v) at room temperature, the probe displayed a strong emission at 496 nm along with a color change from brown-red to yellow. The response was attributed to the reaction of dicyanovinyl groups with hydrazine to afford hydrazone, which was supported by ^{1}H NMR and HRMS. The detection limit of **Che-Dcv** for hydrazine was estimated to be as low as 1.08 ppb and good selectivity over amines including hydroxylamine was observed. Then, the potential of probe-coated test papers to detect hydrazine in solution and vapor phase was demonstrated. Moreover, the bioimaging of hydrazine in living H1975 cells was performed successfully.

Introduction

As a well-known diamine with strong basicity, reducing power and nucleophilicity, hydrazine (N_2H_4) has been widely used in many fields for a long time.[1] It can serve as high-energy rocket propellant,[2] fuel for cells,[3] corrosion inhibitor[4] and blowing agent,[5] it can also be used as the intermediate to produce pharmaceuticals, insecticides, antioxidants, textile dyes, photographic developers and polymers.[6,7] On the other hand, hydrazine is notorious for its toxicity to human beings and the environment.[8–10] In accordance with the U.S. Environmental Protection Agency, the allowable limit of hydrazine in drinking water is 10 ppb.[11]

Apart from the synthetic hydrazine which may pose a potential threat to the environment, hydrazine may also be generated as a byproduct by certain yeasts and some nitrogen fixing bacteria.[12] Moreover, the endogenous aminoacylase may induce a hydrolytic cleavage of some drugs such as isoniazid and pasiniazide to liberate free hydrazine in animal or human body as a toxic metabolite.[13,14] Considering the carcinogenic and mutagenic properties of hydrazine, it is highly desirable to detect hydrazine in both environmental and biological samples sensitively and selectively.

Among various analytic methods for hydrazine, fluorescent techniques are extremely attractive because of their high sensitivity, easy implementation, biocompatibility and real-time detection. The past decade has witnessed the thriving of fluorescent probes for hydrazine detection, and the design strategies as well as applications of various fluorescent probes have been extensively reviewed recently.[15,16]

Generally, recognition site and fluorophore are two requisites for a reaction-based small molecule fluorescent probe, the former primarily determines the selectivity of the probe, and the latter determines the optical properties of the probe, such as the excitation/emission wavelength, Stokes shift, quantum yield, and sensitivity. It is noticeable that even attachment of the same recognition site to different fluorophores can result in distinctive differences in the overall behavior of the probes.[15] For example, when acetate, the simplest and widely exploited recognition site for hydrazine was connected to different fluorophores such as flavonoid,[17] resorufin[18] and cyanine[19] to afford different probes, the detection limits of hydrazine were 320 ppb, 26.2 ppb and 0.81 ppb respectively, and the solubility, emission wavelength, response time and selectivity toward hydrazine varied greatly. Hence, the design or selection of fluorophore is pivotal to construct an efficient probe.

Till now, a wide diversity of fluorophores such as cyanine,[19,20] hemicyanine,[21,22] BODIPY,[23,24] fluorescein,[25,26] benzothiazole,[27,28] coumarin,[29,30] naphthalimide,[31,32] quinolone,[33] phenothiazine,[34] benzimidazole,[35] phenanthroimidazole,[36] pyrene[37] and tetraphenylethylene[38] have been applied in the manufacturing of fluorescent probes for hydrazine detection and different properties and applications have been demonstrated. Unlike the aforementioned classical fluorophores with at least one aromatic or heteroaromatic ring, herein, we report the synthesis

[a]*School of Chemical Engineering, Sichuan University, Chengdu 610065, P. R. China. E-mail: hwc@scu.edu.cn*

[b]*West China School of Pharmacy, Sichuan University, Chengdu 610041, P. R. China*

[c]*State Key Laboratory of Biotherapy and Cancer Center, West China Hospital, West China Medicinal School, Sichuan University, Chengdu 610041, P. R. China. E-mail: yangli@scu.edu.cn*

and application of a novel fluorescent probe (**Che-Dcv**) with a unique conjugated π-structure as the fluorophore. As for the recognition site for hydrazine, dicyanovinyl was selected because it has been successfully used to fabricate various fluorescent probes owning to its strong electron-withdrawing property and specific reactivity toward hydrazine.[29,34,38–46]

Thus, the dimethylamino group and dicyanovinyl groups connected to the 1,4-cyclohexadiene ring act as the electro-donating group and electro-withdrawing groups respectively, providing a typical donor–π–acceptor (D–π–A) system. When the two dicyanovinyl groups reacted with hydrazine in solution to afford hydrazone, the fluorometric properties changed markedly *via* an intramolecular charge transfer (ICT) mechanism, leading to the sensitive and selective responses observed. Moreover, applications of the probe on test strip experiment and bioimaging of hydrazine in living cells have been successfully demonstrated.

Materials and methods

Materials and instruments

All the chemicals and solvents were of analytical grade and purchased from commercial suppliers. They were used as received without further purification unless otherwise stated. As for the selectivity study, KCl, CaCl$_2$, FeCl$_3$, CuSO$_4$, MgSO$_4$, NaCl, Na$_2$SO$_4$, NaNO$_2$, Na$_2$CO$_3$, NH$_4$Cl, ammonia, hydroxylamine, diethylamine, ethylenediamine, aniline, thiourea, L-Ile, L-Phe, L-Pro, L-His, L-Arg, L-Lys, isoniazid, acethydrazide were used to prepare the stock solutions. Ultrapure water was purified from Millipore water purification system and used throughout all the experiments. Silica gel P60 (Qingdao, mesh number 200–300) was used for column chromatography. ^{1}H NMR and ^{13}C NMR spectra were recorded on a Bruker 400 M instrument and chemical shifts were given in ppm. Mass spectra (ESI) were measured on a Finnigan LCQ DECA spectrometer. UV-vis and fluorescence spectra were recorded on a SHIMADZU UV-2450 spectrophotometer and a VARIAN Cary Eclipse FL1003 M013 spectrometer respectively. The pH value was measured using a pHS-25 digital pH meter. H1975 cells were obtained from American Type Culture Collection (ATCC) and their fluorescence images were captured with a ZEISS LSM 880 Laser scanning confocal microscope.

Synthesis

Probe **Che-Dcv** was synthesized *via* a three-step procedure as depicted in Scheme 1. Structural identification of the intermediates and probe was confirmed by ^{1}H NMR, ^{13}C NMR and HRMS spectroscopy (Fig. S1–S7†).

Synthesis of compound 1. 5,5-Dimethyl-1,3-cyclohexanedione (4.20 g, 30.00 mmol) and N,N-dimethylformamide (2.85 g, 39.04 mmol) were dissolved in CH$_2$Cl$_2$ (10 mL) at 0 °C, then a solution of oxalyl chloride (4.92 g, 39.07 mmol) in CH$_2$Cl$_2$ (5 mL) was added dropwise. After the addition, the solution was stirred at room temperature for 2 h. Subsequently, the mixture was poured into ice water (50 mL) and extracted with CH$_2$Cl$_2$ (20 mL × 4). After washing with saturated saline, drying over anhydrous sodium
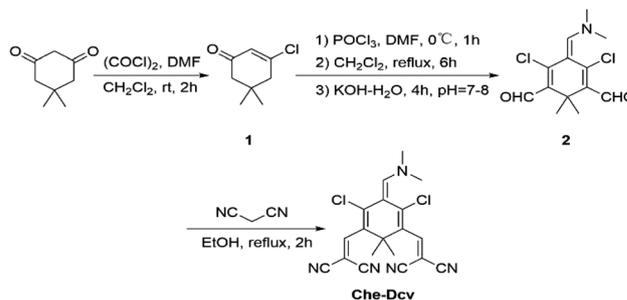
Scheme 1 Synthetic route of **Che-Dcv**.

sulfate and filtration, the combined organic phase was evaporated under reduced pressure to give compound **1** as a light yellow oily liquid (4.36 g, 92.0%). ^{1}H NMR (400 MHz, CDCl$_3$) δ 6.14 (s, 1H), 2.49 (s, 2H), 2.18 (s, 2H), 1.02 (s, 6H).

Synthesis of compound 2. Phosphorus oxychloride (10.00 g, 65.35 mmol) was added dropwise to a solution of N,N-dimethylformamide (8.04 g, 110.14 mmol) in CH$_2$Cl$_2$ (10 mL) with stirring at 0 °C and the mixture was further stirred for 1 h. After the addition of a solution of compound **1** (3.48 g, 22.03 mmol) in CH$_2$Cl$_2$ (10 mL), the mixture was refluxed for 6 h. Then, the reactant was cooled to room temperature and poured into ice water (30 mL), 5 M KOH solution was added dropwise to adjust the pH to 7.0–8.0. The mixture was stirred for another 4 h at room temperature and extracted with CH$_2$Cl$_2$ (40 mL × 4). The combined organic phase was washed with saturated saline twice, dried over anhydrous sodium sulfate, filtered and concentrated under reduced pressure to obtain an orange oily liquid. The crude product was purified by column chromatography on silica gel (cyclohexane : ethyl acetate = 6 : 1, v/v) to afford compound **2** as an orange powder (1.91 g, 30.0%). ^{1}H NMR (400 MHz, CDCl$_3$) δ 10.12 (s, 2H), 7.52 (s, 1H), 3.19 (s, 6H), 1.65 (s, 6H). ^{13}C NMR (100 MHz, DMSO-d_6) δ 189.7, 154.5, 146.0, 129.4, 99.8, 45.9, 42.4, 24.8. HRMS m/z: calculated for [C$_{13}$H$_{15}$Cl$_2$NO$_2$ + Na]$^+$, 310.0378, found: 310.0376.

Synthesis of probe Che-Dcv. A solution of malononitrile (0.46 g, 6.97 mmol) in EtOH (5 mL) was added dropwise to the solution of compound **2** (1.00 g, 3.48 mmol) in EtOH (15 mL) at room temperature. After refluxing for 2 h and cooling, the reactant was concentrated under reduced pressure and the obtained solid was further purified by column chromatography on silica gel (cyclohexane : ethyl acetate = 10 : 1, v/v) to afford probe **Che-Dcv** as a black powder (0.42 g, 36.0%). ^{1}H NMR (400 MHz, CDCl$_3$) δ 7.52 (s, 1H), 7.40 (s, 2H), 3.27 (s, 6H), 1.30 (s, 6H). ^{13}C NMR (100 MHz, CDCl$_3$) δ 189.8, 157.9, 152.6, 113.1, 112.4, 102.6, 90.2, 45.7, 44.5, 26.5. HRMS m/z: calculated for [C$_{19}$H$_{15}$Cl$_2$N$_5$ + Na]$^+$, 406.0602, found: 406.0607.

Spectral measurements

For UV-vis and fluorescence titrations, stock solutions of probe **Che-Dcv** (50 μM) and N$_2$H$_4$ (10 mM) were prepared in DMSO and ultrapure water respectively. In titration experiment, a typical test sample was prepared by mixing 0.4 mL probe stock solution and certain amount of N$_2$H$_4$ stock solution in a test

tube, then diluting to 2.0 mL with PBS buffer (pH = 7.4, 10 mM), the final concentration of probe **Che-Dcv** was 10 μM. After the resulting solution was incubated at 25 °C for 15 min, UV-vis absorption and fluorescence spectra (λ_{ex} = 350 nm or 480 nm, slit width: d_{ex}/d_{em} = 10/10 nm or 20/20 nm) were recorded. The effect of different pH (3.0–9.0) was recorded by fluorescence spectra (λ_{ex} = 350 nm, slit width: d_{ex}/d_{em} = 10/10 nm).

Selectivity study

Parallel experiments were carried out to investigate the selectivity of probe **Che-Dcv** toward hydrazine over other interfering analytes such as cations (K^+, Ca^{2+}, Fe^{3+}, Cu^{2+}, Mg^{2+}, NH_4^+), anions (Cl^-, SO_4^{2-}, NO_2^-, CO_3^{2-}), amino acids (L-Ile, L-Phe, L-Pro, L-His, L-Arg, L-Lys), amines (ammonia, hydroxylamine, diethylamine, ethylenediamine, aniline, thiourea) and hydrazine derivatives (isoniazid, acethydrazide). Stock solutions of these interfering analytes (40 mM) were prepared in DMSO or ultrapure water and then diluted with PBS buffer (containing 20% DMSO, pH = 7.4, 10 mM). The final concentration of interfering analytes was 400 μM while the concentration of hydrazine was 200 μM.

Detection of hydrazine by test strips

Filter paper strips were soaked in a DMSO solution of probe **Che-Dcv** (1 mM) for 30 s and then dried in air. When the probe-coated test strips were used to detect hydrazine in vapor phase, they were placed to cover brown bottles containing different concentrations of N_2H_4 (0.01–40%) or saturated vapor of interfering substances (HCHO, Et_3N, CO_2 and HCl) for 30 min. When they were used to detect of hydrazine in aqueous solution, they were infiltrated in solutions of different concentrations of N_2H_4 (0.01–40%) for 10 s and then dried in air. All the operations were carried out in a fume hood at room temperature and the treated test strips were observed under natural light or UV lamp (365 nm).

Cell imaging experiments

H1975 cells were cultured in Dulbecco's Modified Eagle's Medium (DMEM, pH = 7.2–7.4) supplemented with 10% fetal bovine serum (FBS) in a 5% CO_2 atmosphere at 37 °C. Before cell imaging experiments, H1975 cells were seeded in 96-well plates and incubated for 24 h. The cytotoxicity of **Che-Dcv** was evaluated with a standard MTT assay. H1975 cells were treated with 10 μL increasing concentrations of probe (0, 1, 2, 4, 8, 16 and 32 μM) for 2 h followed by 10 μL MTT for another 24 h, the absorbance at 803 nm of each well was measured by a microplate reader. Finally, the cell viability was calculated. For fluorescence microscopy imaging experiment, H1975 cells were incubated with 10 μM **Che-Dcv** (0.05% DMSO–PBS, v/v) for 4 h at 37 °C and slightly rinsed 3 times with PBS buffer. Then, the pretreated cells were further incubated with 50 μM N_2H_4 for another 15 min, fixed with 4% paraformaldehyde for 5 min and washed 3 times with PBS buffer. At last, the laser scanning confocal microscopy images were recorded (λ_{ex} = 480 nm, λ_{em} = 750–850 nm and λ_{ex} = 350 nm, λ_{em} = 440–630 nm).

Result and discussion

Design and synthesis of the probe

Although various fluorophores have been used to prepare fluorescent probes for hydrazine detection, new fluorophores with unique optical properties are still in urgent demand. Under the action of DMF–$POCl_3$, cyclohexanone could be converted to 2-chloro-3-(hydroxymethylene)-1-cyclohexene-1-carboxaldehyde followed by reaction with substituted indolenine quaternary ammonium salts to generate various heptamethine cyanines.[47,48] Inspired by this strategy, we selected cyclohexanediones as the starting material to explore their potential of constructing new fluorophores. As a consequence, 5,5-dimethyl-1,3-cyclohexanedione reacted with DMF and oxalyl chloride to obtain β-halo-α,β-unsaturated ketone **1**.[49] Then, **1** was transformed to **2** under the action of DMF–$POCl_3$.[50] It should be noted that dimethyl attached to the 1,4-cyclohexadiene ring prevented the aromatization of **2** to form 2,4-dichlorobenzene – 1,3,5-tricarbaldehyde, thus forming a unique nonaromatic conjugated structure with one dimethylamino group and two aldehyde groups. Finally, condensation of **2** with malononitrile in ethanol afforded probe **Che-Dcv**.
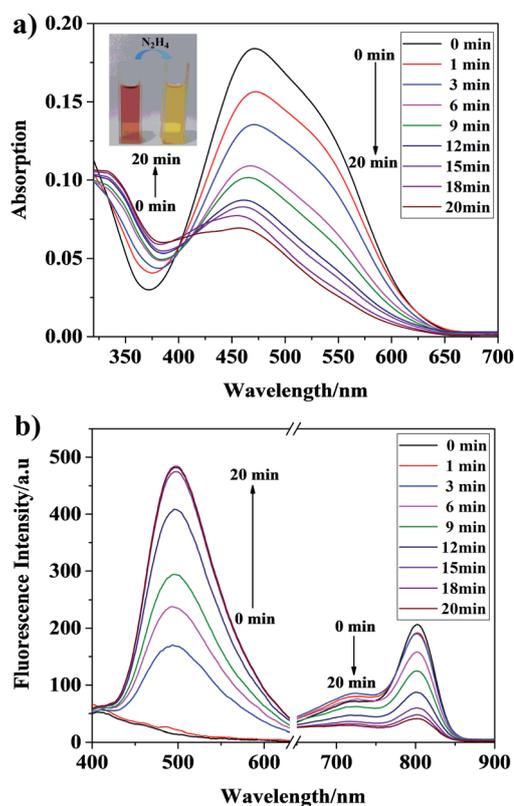

Fig. 1 Absorption spectral (a) and fluorescence spectral (b) changes of probe **Che-Dcv** (10 μM) in the absence or presence of N_2H_4 (200 μM) in 20% DMSO–PBS buffer (pH = 7.4, 10 mM, v/v) over time at 25 °C (λ_{ex} = 480 nm, λ_{em} = 803 nm and λ_{ex} = 350 nm, λ_{em} = 496 nm). Inset: color changes from brown-red to yellow of the probe **Che-Dcv** with the addition of N_2H_4 under natural light.
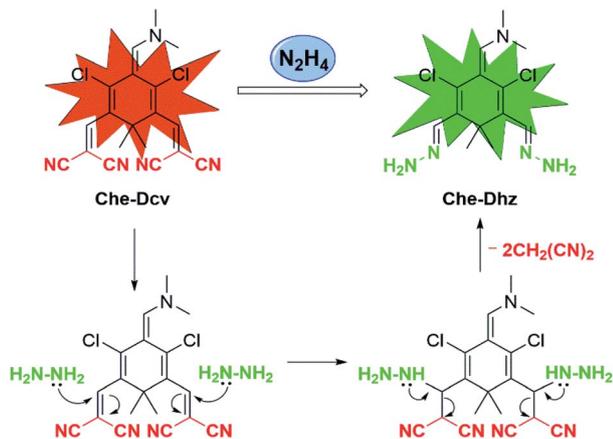
Spectral response of probe to hydrazine

Time-dependent absorption and fluorescence spectral responses of **Che-Dcv** (10 μM) towards hydrazine (200 μM) in 20% DMSO–PBS buffer (pH = 7.4, 10 mM, v/v) were investigated and the results were illustrated in Fig. 1a. It could be seen that the free probe **Che-Dcv** showed a broad absorption band centered at 470 nm. Upon addition of 200 μM hydrazine, the maximum absorption band gradually decreased, while the absorption band at 340 nm increased very slightly. Meanwhile, the color of the solution changed from brown-red to yellow under natural light, suggesting that hydrazine could be detected by the naked-eye (Fig. 1a inset). On the other hand, the fluorescence emission at 803 nm (λ_{ex} = 480 nm) decreased gradually while the fluorescence emission at 496 nm (λ_{ex} = 350 nm) increased markedly after the addition of hydrazine. As shown in Fig. 1b, the equilibrium was reached within 15 min and nearly no further fluorescence enhancement at 496 nm could be observed afterwards. Additionally, the Stokes shift of **Che-Dcv** was calculated to be 146 nm when excited at 350 nm.

Sensing mechanism

Based on the structural properties of **Che-Dcv** and reported literatures,[29,34,38–46] we speculate that dicyanovinyl groups in **Che-Dcv** serve as not only the electron-withdrawing groups of the typical D–π–A structure but also the recognition sites for hydrazine. Accordingly, the proposed sensing mechanism is illustrated in Scheme 2. Upon the addition of hydrazine, the dicyanovinyl groups in **Che-Dcv** were attacked and the product hydrazone (**Che-Dhz**) was generated, thus triggering the disappearance of red fluorescence and appearance of strong green fluorescence observed.

To further verify the detection mechanism, ^{1}H NMR spectroscopic analysis of **Che-Dcv** was carried out before and after the addition of hydrazine. As shown in Fig. S8,† the protons of methyl (Ha) and dimethylamine (Hb) groups in **Che-Dcv** appeared at 1.25 and 3.25 ppm respectively. Upon addition of hydrazine to the DMSO-d_6 solution of **Che-Dcv**, the proton signal of the methyl groups (Ha at δ 1.25 ppm) was divided into two single signals (Ha′ at δ 1.17 and Ha″ at 1.61 ppm) and the proton signal of the dimethylamine group shifted from 3.25 (Hb) to 2.19 ppm (Hb′). At the same time, a new single peak appeared at 5.82 ppm (He′, =N–NH₂) indicated the formation of hydrazone. Additionally, when the reaction mixture of **Che-Dcv** and enough hydrazine was subjected to ESI-MS analysis, a peak at *m/z* 333.1359 which belonged to [**Che-Dhz** + NH₄]⁺ (calculated: 333.1361) could be found (Fig. S9†). Taken together, these experimental results proved the formation of **Che-Dhz** and the sensing mechanism proposed.

Sensitive detection of hydrazine

To investigate the sensitivity of **Che-Dcv**, fluorescence titration experiments of the probe with hydrazine were performed. As shown in Fig. 2a, the fluorescence intensity at 496 nm increased gradually with increasing hydrazine concentration. A good linear relationship (R^2 = 0.9932) was observed between the fluorescence intensity and hydrazine concentration in the range of 0–200 μM (Fig. 2b). Under the experimental conditions, the detection limit (3σ/slope) of probe **Che-Dcv** towards hydrazine was determined to be 1.18 ppb which was much lower than the TLV (10 ppb) recommended by the EPA. The observed low detection limit indicated the potential of **Che-Dcv** for sensitive detection of hydrazine in aqueous solution.
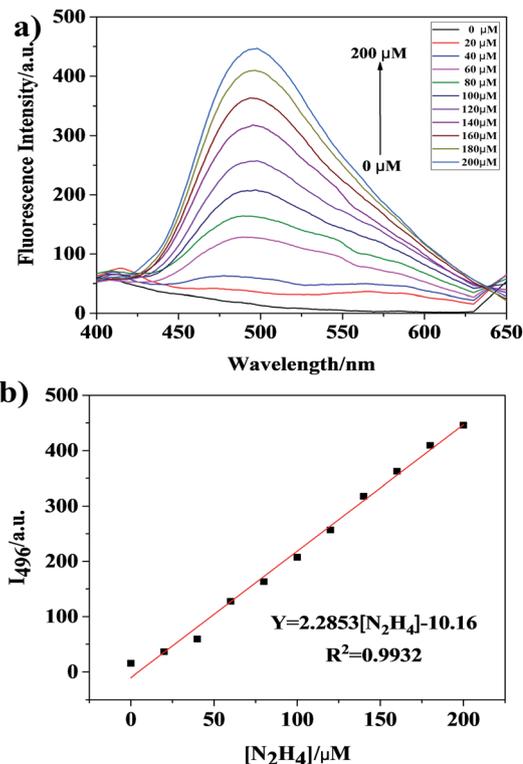

Fig. 2 (a) Fluorescence spectra of **Che-Dcv** (10 μM) upon the addition of increasing concentrations of hydrazine (0, 20, 40, 60, 80, 100, 120, 140, 160, 180, 200 μM) in 20% DMSO–PBS buffer (pH = 7.4, 10 mM, v/v) at 25 °C (λ_{ex} = 350 nm, λ_{em} = 496 nm). (b) Fluorescence intensity changes of **Che-Dcv** at 496 nm as a function of hydrazine concentration.

Scheme 2 Proposed sensing mechanism of probe **Che-Dcv** for detection of N₂H₄.

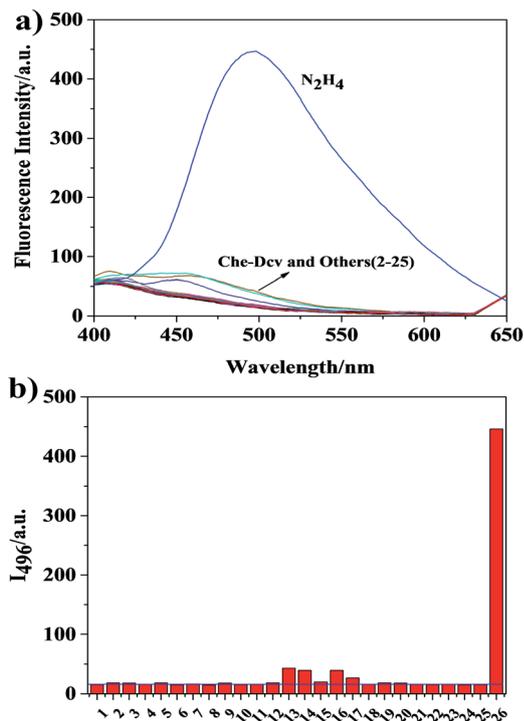Fig. 3 (a) Fluorescence responses and (b) fluorescence enhancements at 496 nm of **Che-Dcv** (10 μM) upon addition of 20 equiv. of N_2H_4 and 40 equiv. of interfering analytes ((1) **Che-Dcv**; (2) K^+; (3) Ca^{2+}; (4) Fe^{3+}; (5) Cu^{2+}; (6) Mg^{2+}; (7) Cl^-; (8) SO_4^{2-}; (9) NO_2^-; (10) CO_3^{2-}; (11) NH_4^+; (12) ammonia; (13) hydroxylamine; (14) diethylamine; (15) ethylenediamine; (16) aniline; (17) thiourea; (18) L-Ile; (19) L-Phe; (20) L-Pro; (21) L-His; (22) L-Arg; (23) L-Lys; (24) isoniazid; (25) acetylhydrazine; (26) N_2H_4). λ_{ex} = 350 nm, λ_{em} = 496 nm.

Selectivity studies

To evaluate the selectivity of **Che-Dcv** toward hydrazine, the fluorescence responses of the probe in the presence of various interfering analytes were measured. As shown in Fig. 3, environmentally and biologically important ions (K^+, Ca^{2+}, Fe^{3+}, Cu^{2+}, Mg^{2+}, NH_4^+, Cl^-, SO_4^{2-}, NO_2^-, CO_3^{2-}), amino acids (L-Ile, L-Phe, L-Pro, L-His, L-Arg, L-Lys), amines (ammonia, ethylenediamine) and hydrazine derivatives (isoniazid, acethydrazide) resulted in virtually no effect on the fluorescence of **Che-Dcv**. Only hydroxylamine, diethylamine, aniline and thiourea led to observable enhancement of fluorescence intensity, possibly due to their similar structures and reactivities with hydrazine. In contrast, hydrazine caused a significant increase (33 times) in fluorescence intensity of **Che-Dcv** in PBS buffer (containing 20% DMSO, pH = 7.4, 10 mM). All the results demonstrated the good specificity of **Che-Dcv** for practical detection of hydrazine in real environmental and biological samples.

Effect of pH

It is well known that the specific reaction of hydrazine and dicyanovinyl group results from the strong nucleophilicity of hydrazine, we envision that the protonated form of hydrazine may hinder its reaction with dicyanovinyl group. Hence, it is necessary to explore the effect of pH on the fluorescence
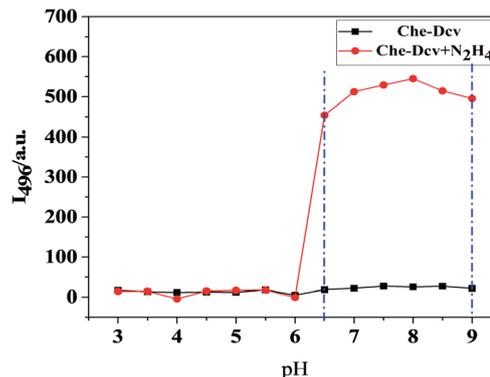

Fig. 4 The effect of pH (3.0–9.0) on the fluorescence intensity at 496 nm of probe **Che-Dcv** (10 μM) in the absence or presence of N_2H_4 (200 μM).

response of **Che-Dcv** to hydrazine. As shown in Fig. 4, the free probe **Che-Dcv** displayed almost no fluorescence at 496 nm in the wide pH range of 3.0–9.0.

After the addition of 20 equiv. of hydrazine, the fluorescence intensity remained unchanged in the pH range of 3.0–6.0. When the pH value was raised to 6.5, the fluorescence intensity increased dramatically owning to the deprotonation of protonated hydrazine and the following reaction with dicyanovinyl groups. And in the pH range of 6.5–9.0, relatively stable fluorescence intensity was observed, indicating the potential of **Che-Dcv** to detect hydrazine in real samples, especially the biological samples.

Detection of hydrazine by test strips

Encouraged by the high sensitivity and selectivity of probe **Che-Dcv**, we evaluated its potential for on-site visual detection of hydrazine in vapor phase or aqueous solution using probe-coated test papers. As shown in Fig. 5, the color of the test strips covered on the top of bottles changed from brown to white with the increasing concentration of hydrazine contained in the bottle, at the same time, the color change from dark purple to blue under UV lamp (365 nm) was observed. By
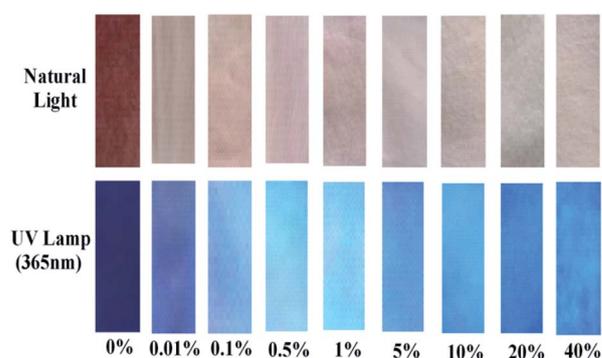

Fig. 5 Color changes of **Che-Dcv**-coated test strips before and after exposure to hydrazine vapors equilibrated with different concentrations of hydrazine (0, 0.01%, 0.1%, 0.5%, 1%, 5%, 10%, 20%, 40%, w/w) under natural light and UV lamp (365 nm).
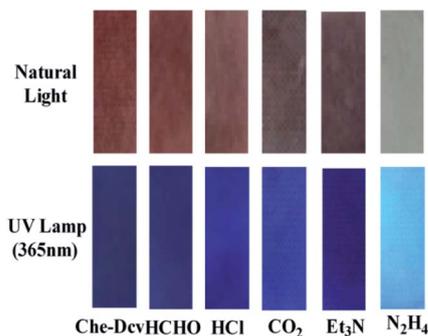
Fig. 6 Color changes of **Che-Dcv**-coated test strips before and after exposure to different interfering gases (HCHO, Et$_3$N, CO$_2$, HCl) under natural light and UV lamp (365 nm).
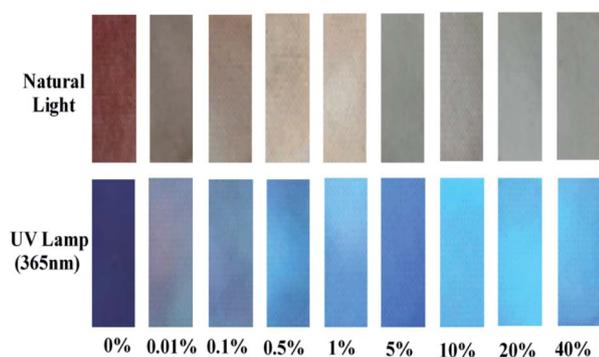

Fig. 7 Color changes of **Che-Dcv**-coated test strips after exposure to different concentrations of hydrazine aqueous solution (0, 0.01%, 0.1%, 0.5%, 1%, 5%, 10%, 20%, 40%, w/w) under natural light and UV lamp (365 nm).

contrast, the color of test strips remained almost unchanged after exposure to HCHO, HCl, CO$_2$ and Et$_3$N under either natural or UV light (Fig. 6). Then, the probe-coated test papers were immersed into hydrazine solutions (0.01–40%, w/w) and viewed after drying in the air. As illustrated in Fig. 7, the gradual color changes from brown to white under natural light and from dark purple to blue under UV light were observed. Taken together, the concentration of hydrazine in a sample could be roughly estimated according to the color change of **Che-Dcv**-coated test strips, providing an easy-to-use method for on-site detection of hydrazine in either vapor phase or aqueous solution.

Cell imaging of hydrazine in living cells

To evaluate the cytotoxicity of probe **Che-Dcv**, standard MTT assays were performed in H1975 cells and the results were illustrated in Fig. S10.† After the H1975 cells were incubated with increasing concentrations of **Che-Dcv** (0, 1, 2, 4, 8, 16 and 32 μM) for 24 h, the cell viability declined slowly. And the cell viability was still about 80% even the probe concentration was as high as 32 μM. These results suggested that **Che-Dcv** had good biocompatibility with living cells.

Then, the ability of probe **Che-Dcv** for bioimaging of hydrazine in living cells was tested. As shown in Fig. 8, H1975 cells
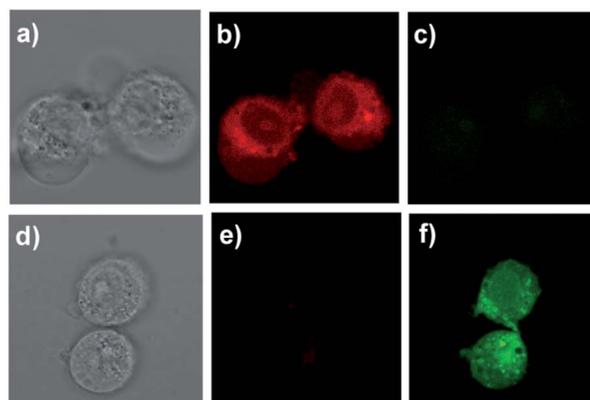

Fig. 8 Confocal fluorescence images of H1975 cells treated with **Che-Dcv** (10 μM) in the absence (a, b and c) or presence (d, e and f) of hydrazine (50 μM). (a and d): bright field images; (b and e): red fluorescent channel ($\lambda_{ex} = 480$ nm, $\lambda_{em} = 750$–850 nm); (c and f): green fluorescent channel ($\lambda_{ex} = 350$ nm, $\lambda_{em} = 440$–630 nm), scale bar: 5 μm.

treated with 10 μM **Che-Dcv** for 4 h displayed an intense red fluorescence and a weak green fluorescence. When the **Che-Dcv**-pretreated cells were further cultured with 50 μM hydrazine for 15 min, the red fluorescence was diminished while the green fluorescence was enhanced significantly. These results were in accordance with the fluorescent behavior of **Che-Dcv** in solution and demonstrated its capability of visualizing hydrazine in living cells.

Conclusion

In summary, a new fluorescent probe **Che-Dcv** was designed and synthesized for the detection of hydrazine. With dicyanovinyl groups as the recognition sites, the probe responded to hydrazine sensitively and selectively with a color change from brown-red to yellow. The Stokes shift was calculated to be 146 nm. After being coated on filter paper strips, probe **Che-Dcv** could achieve on-site detection of hydrazine in either vapor phase or aqueous solution by color and fluorescence changes. In addition, this probe was successfully applied to imaging hydrazine in living H1975 cells. And more importantly, a new type of fluorophore with neither an aromatic nor a heteroaromatic ring is presented in this paper and its potential to fabricate practical fluorescent probes has been demonstrated. This strategy may broaden the scope of fluorophore and make the structures of fluorescent probes more devisable.

Conflicts of interest

There are no conflicts to declare.

Acknowledgements

Notes and references

1 J. Sanabria-Chinchilla, K. Asazawa, T. Sakamoto, K. Yamada, H. Tanaka and P. Strasser, *J. Am. Chem. Soc.*, 2011, **133**, 5425–5431.

2 R. Lan, J. T. S. Irvine and S. Tao, *Int. J. Hydrogen Energy*, 2012, **37**, 1482–1494.

3 A. Serov and C. Kwak, *Appl. Catal., B*, 2010, **98**, 1–9.

4 V. K. Gouda and S. M. Sayed, *Corros. Sci.*, 1973, **13**, 647–652.

5 I. C. Vieira, K. O. Lupetti and O. Fatibello-Filho, *Anal. Lett.*, 2002, **35**, 2221–2231.

6 U. Ragnarsson, *Chem. Soc. Rev.*, 2001, **30**, 205–213.

7 J.-P. Schirmann and P. Bourdauducq, Hydrazine, *Ullmann's Encyclopedia of Industrial Chemistry*, Wiley-VCH Verlag GmbH & Co. KGaA, Weinheim, Germany, 2000.

8 S. Garrod, M. E. Bollard, A. W. Nicholls, S. C. Connor, J. Connelly, J. K. Nicholson and E. Holmes, *Chem. Res. Toxicol.*, 2005, **18**, 115–122.

9 B. Toth, *Cancer Res.*, 1975, **35**, 3693–3697.

10 S. D. Zelnick, D. R. Mattie and P. C. Stepaniak, *Aviat Space Environ. Med.*, 2003, **74**, 1285–1291.

11 US Environmental Protection Agency (EPA), *Integrated Risk Information System (IRIS) on Hydrazine/Hydrazine Sulfate*, National Center for Environmental Assessment, Office of Research and Development, Washington DC, 1999.

12 M. Strous and M. S. Jetten, *Annu. Rev. Microbiol.*, 2004, **58**, 99–117.

13 G. A. Ellard and P. T. Gammon, *J. Pharmacokinet. Biopharm.*, 1976, **4**, 83–113.

14 H. Singh, K. Tiwari, R. Tiwari, S. K. Pramanik and A. Das, *Chem. Rev.*, 2019, **119**, 11718–11760.

15 B. Roy and S. Bandyopadhyay, *Anal. Methods*, 2018, **10**, 1117–1139.

16 S. K. Manna, A. Gangopadhyay, K. Maiti, S. Mondal and A. K. Mahapatra, *ChemistrySelect*, 2019, **4**, 7219–7245.

17 B. Liu, Q. Liu, M. Shah, J. Wang, G. Zhang and Y. Pang, *Sens. Actuators, B*, 2014, **202**, 194–200.

18 M. G. Choi, J. O. Moon, J. Bae, J. W. Lee and S.-K. Chang, *Org. Biomol. Chem.*, 2013, **11**, 2961–2965.

19 C. Hu, W. Sun, J. Cao, P. Gao, J. Wang, J. Fan, F. Song, S. Sun and X. Peng, *Org. Lett.*, 2013, **15**, 4022–4025.

20 Z. Lu, W. Fan, X. Shi, Y. Lu and C. Fan, *Anal. Chem.*, 2017, **89**, 9918–9925.

21 J. Zhang, L. Ning, J. Liu, J. Wang, B. Yu, X. Liu, X. Yao, Z. Zhang and H. Zhang, *Anal. Chem.*, 2015, **87**, 9101–9107.

22 Y. He, Z. Li, B. Shi, Z. An, M. Yu, L. Wei and Z. Ni, *RSC Adv.*, 2017, **7**, 25634–25639.

23 B. Li, Z. He, H. Zhou, H. Zhang, W. Li, T. Cheng and G. Liu, *Dyes Pigm.*, 2017, **146**, 300–304.

24 A. K. Mahapatra, R. Maji, K. Maiti, S. K. Manna, S. Mondal, S. S. Ali, S. Manna, P. Sahoo, S. Mandal, M. R. Uddin and D. Mandal, *RSC Adv.*, 2015, **5**, 58228–58236.

25 S. Goswami, K. Aich, S. Das, S. B. Roy, B. Pakhira and S. Sarkar, *RSC Adv.*, 2014, **4**, 14210–14214.

26 S. Goswami, S. Paul and A. Manna, *New J. Chem.*, 2015, **39**, 2300–2305.

27 C. Liu, F. Wang, T. Xiao, B. Chi, Y. Wu, D. Zhu and X. Chen, *Sens. Actuators, B*, 2018, **256**, 55–62.

28 Y. Wang, H. Xiang, R. Zhao and C. Huang, *Analyst*, 2018, **143**, 3900–3906.

29 S. Goswami, S. Das, K. Aich, D. Sarkar and T. K. Mondal, *Tetrahedron Lett.*, 2014, **55**, 2695–2699.

30 S.-H. Guo, Z.-Q. Guo, C.-Y. Wang, Y. Shen and W.-H. Zhu, *Tetrahedron*, 2019, **75**, 2642–2646.

31 Y. Hao, Y. Zhang, K. Ruan, W. Chen, B. Zhou, X. Tan, Y. Wang, L. Zhao, G. Zhang, P. Qu and M. Xu, *Sens. Actuators, B*, 2017, **244**, 417–424.

32 L. Cui, C. Ji, Z. Peng, L. Zhong, C. Zhou, L. Yan, S. Qu, S. Zhang, C. Huang, X. Qian and Y. Xu, *Anal. Chem.*, 2014, **86**, 4611–4617.

33 Q. Wu, J. Zheng, W. Zhang, J. Wang, W. Liang and F. J. Stadler, *Talanta*, 2019, **195**, 857–864.

34 M. Sun, J. Guo, Q. Yang, N. Xiao and Y. Li, *J. Mater. Chem. B*, 2014, **2**, 1846–1851.

35 J. Cui, L. Cao, G. Wang, W. Ji, H. Nie, C. Yang and X. Zhang, *Anal. Methods*, 2019, **11**, 5023–5030.

36 F. Ali, H. A. Anila, N. Taye, D. G. Mogare, S. Chattopadhyay and A. Das, *Chem. Commun.*, 2016, **52**, 6166–6169.

37 B. Roy, S. Halder, A. Guha and S. Bandyopadhyay, *Anal. Chem.*, 2017, **89**, 10625–10636.

38 R. Zhang, C.-J. Zhang, Z. Song, J. Liang, R. T. K. Kwok, B. Z. Tang and B. Liu, *J. Mater. Chem. C*, 2016, **4**, 2834–2842.

39 J. Fan, W. Sun, M. Hu, J. Cao, G. Cheng, H. Dong, K. Song, Y. Liu, S. Sun and X. Peng, *Chem. Commun.*, 2012, **48**, 8117–8119.

40 S. Goswami, S. Paul and A. Manna, *RSC Adv.*, 2013, **3**, 18872–18877.

41 X.-X. Zheng, S.-Q. Wang, H.-Y. Wang, R.-R. Zhang, J.-T. Liu and B.-X. Zhao, *Spectrochim. Acta, Part A*, 2015, **138**, 247–251.

42 S. I. Reja, N. Gupta, V. Bhalla, D. Kaur, S. Arora and M. Kumar, *Sens. Actuators, B*, 2016, **222**, 923–929.

43 Shweta, A. Kumar, Neeraj, S. K. Asthana, A. Prakash, J. K. Roy, I. Tiwari and K. K. Upadhyay, *RSC Adv.*, 2016, **6**, 94959–94966.

44 X. Yang, Y. Liu, Y. Wu, X. Ren, D. Zhang and Y. Ye, *Sens. Actuators, B*, 2017, **253**, 488–494.

45 Y.-D. Lin and T. J. Chow, *RSC Adv.*, 2013, **3**, 17924–17929.

46 J. Qiu, Y. Chen, S. Jiang, H. Guo and F. Yang, *Analyst*, 2018, **143**, 4298–4305.

47 N. Narayanan and G. Patonay, *J. Org. Chem.*, 1995, **60**, 2391–2395.

48 S. Luo, X. Tan, S. Fang, Y. Wang, T. Liu, X. Wang, Y. Yuan, H. Sun, Q. Qi and C. Shi, *Adv. Funct. Mater.*, 2016, **26**, 2826–2835.

49 R. E. Mewshaw, *Tetrahedron Lett.*, 1989, **30**, 3753–3756.

50 A. R. Katritzky and C. M. Marson, *J. Org. Chem.*, 1987, **52**, 2726–2730.